Acta Montanistica Slovaca
ISSN 1335-1788
actamont.tuke.sk

Hazard Assessment of Bedrock Discontinuities Using Integration of Structural Data and Geotechnical Characterization: A Case Study from the Northern Galala Plateau, Egypt

Abdelaziz El SHINAWI, Fares KHEDR[2] and Ahmed HENAISH[3]

Authors' affiliations and addresses:
[1] Environmental Geophysics Lab (ZEGL), Department of Geology, Faculty of Science, Zagazig University, Zagazig, Egypt
e-mail: geoabdelaziz@yahoo.com

[2] Department of Geology, Faculty of Science, Suez University, Suez, Egypt
e-mail: fares.khedr@suezuni.edu.eg

[3]Department of Geology, Faculty of Science, Zagazig University, Zagazig, 44519, Egypt
email: ahmed_henaish@zu.edu.eg

***Correspondence:**
Abdelaziz El Shinawi, Environmental Geophysics Lab (ZEGL), Department of Geology, Faculty of Science, Zagazig University, Zagazig, Egypt
e-mail: geoabdelaziz@yahoo.com

Acknowledgement:
We are gratefully acknowledged to the Zagazig University Environmental Geophysics Laboratory (ZEGL), Faculty of science and soil mechanics Lab, faculty of engineering, for helping us to perform the laboratory testing.

How to cite this article:
Shinawi, A.E., Khedr, F. and Henaish, A. (2022). Hazard Assessment of Bedrock Discontinuities Using Integration of Structural Data and Geotechnical Characterization: A Case Study from the Northern Galala Plateau, Egypt. *Acta Montanistica Slovaca*, Volume 27 (2), 446-461.

DOI:
https://doi.org/10.46544/AMS.v27i2.13

Abstract
Discontinuities represent a significant role in the deformation of foundation bedrocks and the stability of many slopes. Moreover, assessing and analyzing the different slope failures through fieldwork and laboratory tests of the intact rock mass is important to determine discontinuities' geometrical and geo-engineering parameters. The Northern Galala Plateau is considered a typical case study of instability problems due to excessive bedrock discontinuities. The present study deals with the mapping and assessment of bedrock (Paleozoic sandstones) discontinuities using structural mapping/analysis and geotechnical qualifications as an integrative approach. The study was started by collecting structural data, joint surveying and delineating fault zones as well as highly fractured zones. In addition, the geotechnical qualifications and stability of slopes were assessed using kinematic analysis and Rock Mass Rating (RMR) of discontinuity sets at the lower slope. Quantitative descriptions and statistical distribution of fractures at the study site were well defined. The kinematic analysis of sandstone bedrock masses revealed wedge and/or toppling failures which are controlled by uncomplimentary discontinuities. As a result, RMR values suggested the majority of foundation bedrock is classified as good rock II category, whereas RMR for the fault zone is classified as fair rock III category. Furthermore, discontinuities could not necessarily lead to instability problems during and after construction. The present study highlights the influence of integration between both structural and geotechnical techniques for suitability assessment in development processes which in turn could provide important keys for decision-makers.

Keywords
Northern Galala; geotechnical assessment; discontinuities; kinematic analysis; joint surveying.

Introduction

Nowadays, urbanization is becoming so quick in mountainous and desert-land areas. The intensive urban growth can enlarge the geo-environmental hazards. Accordingly, the characterization of geologic structures and geotechnical properties of rocks are important for environmental engineering investigations (Peng et al., 2021; El Shinawi& Naymushina, 2015; Kramarenko et al., 2016). From an engineering point of view, the instability problems are generally related to the nature of geological structures and the geotechnical properties of the surrounding rocks (e.g., Ozsan et al., 2007; Koleini & Van, 2010; Alfven, 2015; El Shinawi, 2017; Henaish & Attwa, 2018; El Shinawi et al., 2020; Du et al., 2020; Diet Maio et al., 2020). Consequently, development in mountainous deformed areas should be cautious as rock mass geotechnical properties can be highly affected by the nature and distribution of fractures and faults. Moreover, the nature of the intact rock, the stress field, and the geo-material and mechanical properties are required as detailed information on the discontinuities (Naymushina et al., 2010; Attwa & Shinawi, 2014; Abdelatty et al., 2020; El Shinawi et al., 2021).

The discontinuity is a sharp boundary between two different geologic units on the basis of structural or successive variation between units, such as a stratigraphic contact (i.e., soil and rock) or a structural contact (i. e., fractures and fault zone). The stability of bedrock is variable according to lithological and geological discontinuity as well as geological structures. Understanding the geological and geotechnical properties of the surface and near-surface materials (soil or rocks) and mapping different geological hazards play an essential role in designing engineering structures such as roads, tunnels, and new urban areas in order to avoid any deformations or damage to the constructions. Therefore, development in mountainous structured areas should be cautious as it may be challenging to define the location and width of partly or completely hidden fault zones (Shang et al., 2016; Sari, 2019; Attwa & Henaish, 2018; Attwa et al., 2020; Henaish and Kharbish, 2020). The internal structure of faults is not limited to a simple planar surface but includes a damage zone ranging up to several meters in extent where deformation is complex and widely distributed. Therefore, defining fault zones as well as highly fractured zones is an urgent geotechnical concern to reduce environmental and geo-engineering risks (Duffy et al., 2014; Toké, 2014; Ishii, 2017; Leia, 2017; Kang et al., 2018). At the northwestern margin of the Gulf of Suez rift, the Galala Plateau (Fig. 1) represents one of the southernmost plateaus of the Egyptian unstable shelf. It extends about 100 km from Ain Sukhna at north towards the southeast. This Plateau can be divided into three parts: the Northern Galala Plateau, Wadi Araba and Southern Galala Plateau (Fig. 1).

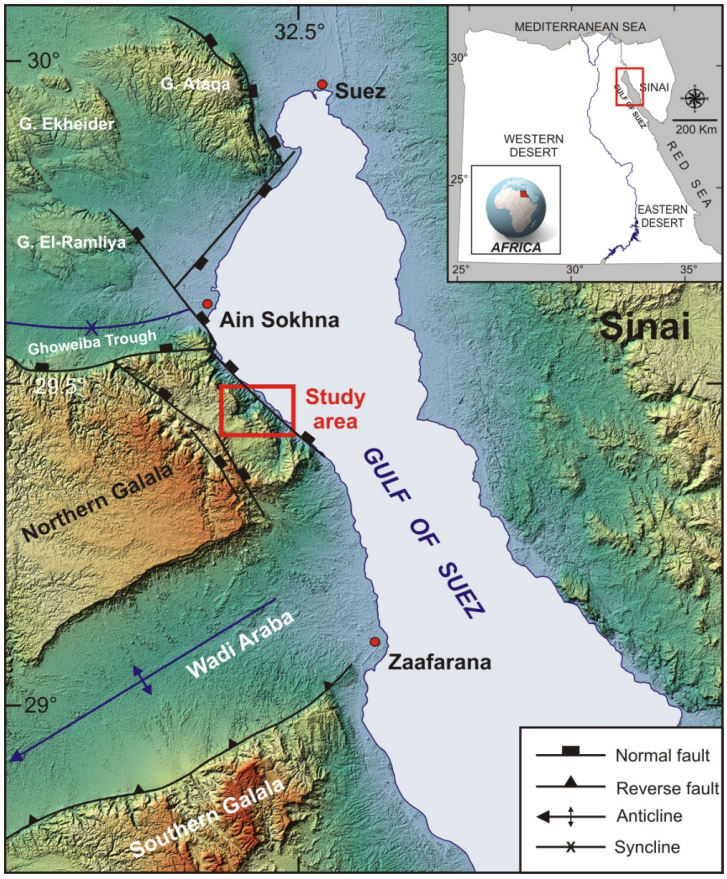

Fig. 1 Digital Elevation Model (DEM) extracted from Shuttle Radar Topography Mission (SRTM) for the Galala Plateaus showing the study area's location.

Recently, the Northern Galala Plateau represents one of the most important locations in Egypt for development projects. However, the Plateau represents a region of low to moderate seismicity (Abou Elenean et al., 2010; Sawires et al., 2016). Hence, defining active fault zones is necessary for future planning to avoid fault rupture hazards. At the eastern scarp of the Northern Galala Plateau, a large number of hotels, resorts and constructions are assembled upon the outcrop of the Paleozoic sandstones, which are considered the foundation bedrock for construction projects (Fig. 2). In addition, ongoing widening and extension processes of the Zafarana-Ain Sukhna road (Fig. 2) are common at the site. As well-observed at the study site, the exposed Paleozoic sandstones are characterized by the abundance of sets of discontinuities (i.e. joints, faults and bedding planes) which can affect the stability of any construction (Fig. 2). Consequently, the present work deals with assessing structural and geo-engineering characteristics of a part of highly deformed Paleozoic sandstone exposed at the Northern Galala Plateau, where faults, fault zones and fractures are dominant.

As a case study, the present work deals with characterizing the geo-engineering situation for a desert-land entry at the northwestern margin of the Gulf of Suez rift, Egypt, where major expansion infrastructure projects are overriding. Occasionally, geotechnical techniques were applied to characterize the geo-engineering characteristics and stability of rock masses. In addition, fractures and fault zones are the main concern for geo-engineering assessment from a structural geology perspective. However, the incorporation of structural and geotechnical data is limited. Consequently, this study is an attempt to find an integrative approach to integrative integrated studies between structural geology and geotechnical engineering. Therefore, we aim to integrate both structural and geotechnical data by (i) assessing the effect of fault zones and fracture sets on rock stability and (ii) evaluating the geotechnical properties of the foundation bedrock with a special focus on the effects on fault zones to rock stability has been considered. This was achieved by assessment of fractures distribution and characteristics in relation to the location of the fault zones. Moreover, geotechnical studies have been applied to intact rocks involved at the fault core of the selected fault zone to examine the effect of the deformation process on the geotechnical properties of rocks.

Fig. 2 Field photos of the Paleozoic sandstone facing the Zaafarana-Ain Sukna road (ZASR) show (a, b) hotels and constructions above the sandstones, (c) rockfall at a slope, (d) highly fractured rock face.

Geologic Settings

The Northern Galala is a high flat-topped plateau and one of the most remarkable topographical features in the northern part of the northern Gulf of Suez rift (Fig.1). The Plateau overlooks the Gulf of Suez and extends for a distance of about 60 km between 50 km south of Suez city in the north and Wadi Araba in the south. The maximum elevation recorded at the Northern Galala Plateau is about 1275 m (above sea level). The Plateau is dissected by several NE as well as NW striking wadis.

Tectonically, the Galala Plateaus are affected by several events which took place throughout Mesozoic-Cenozoic times. The tectonic activity took place in the Early Mesozoic (Tethyan rifting), which revealed a NE-SW to ENE-WSW striking framework of horst and graben structures at the southern Tethyan shelf including Wadi Araba and the Galala Plateaus (Krenkel, 1925; Sahar, 1994; Moustafa & Khalil, 1995; Hussein & Abd-Allah, 2001). The extension was also sustained throughout the Early Cretaceous, which affected the Northern Galala Plateau and Wadi Araba (Hussein & Abd-Allah, 2001). Additionally, during the Late Cretaceous time, convergence between the African and Eurasian plates led to forming compressional structures, forced folds as well as inverted basins along the unstable shelf of Egypt. The evolution of the Galala Plateaus is related to the tectonic activity of the ENE-WSW striking the Wadi Araba Fault (Fig. 1), which represents a part of the Late Cretaceous Syrian Arc Fold Belt (Said, 1990; Krenkel, 1925; Moustafa & Khalil, 1995; Hussein & Abd-Allah, 2001; Henaish, 2018). At the Oligo-Miocene time, the Galala Plateaus were affected by NW-SE striking faults and volcanic intrusions due to the opening of the Gulf of Suez rift. Basaltic lava flows are dominant at the top of the Northern Galala Plateau and at many openings of its valleys (Schütz, 1994; Farouk, 2015; Boukhary, 2019).

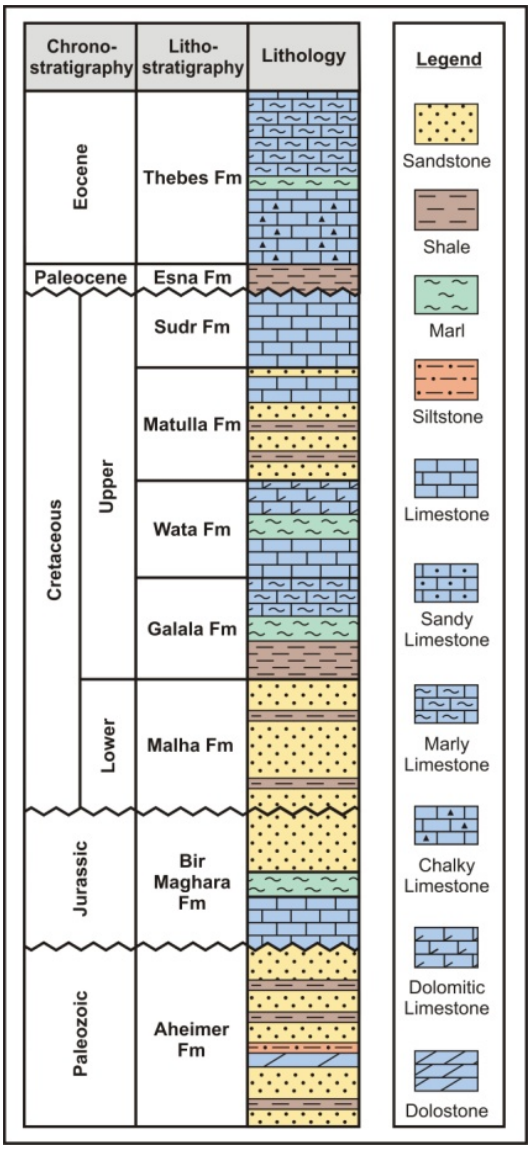

Fig. 3 Generalized stratigraphic column of the Northern Galala Plateau (compiled from, Boukhary, 2019& Abd-Elshafy, 2014; present study).

Generally, the litho-stratigraphic setting of the Northern Galala Plateau is represented by several rock units ranging in age from Paleozoic to Eocene (Fig. 3). The Paleozoic rocks are represented by the sandstones and shales of the Aheimer Formation (Abdallah& Adindani, 1963), which in turn is overlain unconformably by the Jurassic Bir Maghara Formation (Al Far, 1966), which is composed of a series of limestones, marls and sandstones. The Jurassic rocks are followed by the Lower Cretaceous Malha Formation, which is represented by variegated sandstones and shales, which in turn are overlain by the Upper Cretaceous rock units. These units are represented by the Galala Formation (Abdallah & Adindani, 1963), composed of a series of shales, marls and marly limestones is followed by limestones, marls and dolomitic limestones of the Wata Formation. The Wata Formation is overlain by sandstones, shales and limestones of the Matulla Formation, which in turn is followed by the limestones of the Sudr Formation (Ghorab, 1961). Shales of the Paleocene Esna Formation are found in some places in the Upper Cretaceous rocks. All these rocks are capped by Eocene chalky and marly limestones of the Thebes Formation (Said, 1960).

Data and Methods

Discontinuities can affect the stability of any construction and cause instability problems, as those were found in the study site (Aheimer Formation, Ain Sukhna-Zafaraana road). In the present study, a proposed workflow (Fig. 4) integrating outcrop and geotechnical properties is used to avoid the geoenvironmental engineering hazards.

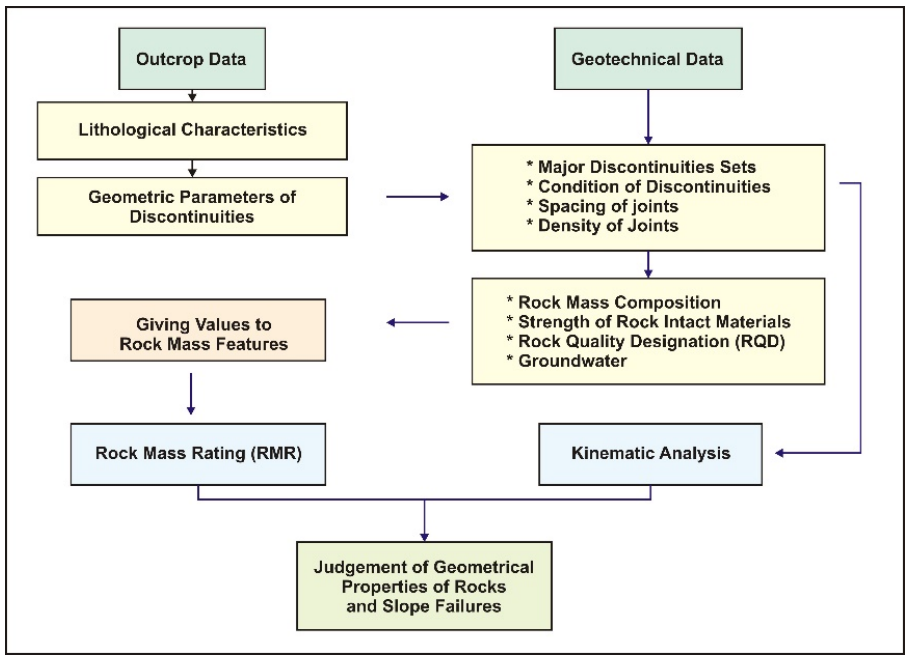

Fig. 4 Workflow and methodologies used in this study.

Lithological Characteristics

The 120 m thick Aheimer Formation (foundation bedrock, Fig. 5) extends for about 10 Km along the foot slope of the Northern Galala Plateau (Fig. 6). The bedding planes of the Aheimer Formation mainly include NW-striking surfaces dipping toward the southwest with dip values that range from 13-25° (Fig. 6). On the basis of lithological composition, the Aheimer Formation is subdivided into three units (Fig. 5). The lower unit is about 38 m thick and comprises cycles of intercalated cross-bedded sandstones and variegated colour fissile shale beds, which reach 120 cm thick. The middle unit thickness measures nearly 24 m and shows a notable increase in carbonate interbeds in the form of dolostone ledges, which reach 50 cm thick, and are intercalated with sandstone, siltstone and mudstone beds. The upper unit is up to 60 m thick and consists of cross-bedded sandstones, dolomitic sandstones and ferruginous mudstone beds.

Structural data

Detailed surface geological mapping was started by studying satellite images (e.g., ETM+ Landsat and Google Earth images) of different scales for the study area. This was followed by field investigations which have been accomplished according to several steps. Firstly, the lithological characteristics of the Aheimer Formation have been studied at different localities in order to figure out aerial extension, thickness and lithological composition. Moreover, strike and dip measurements of bedding planes were taken in order to record the change in attitudes of the strata. Secondly, detailed studies of geological structures affecting the rock unit have been

performed. Both parameters of faults (i.e., the strike, dip value and dip direction) were measured where possible along with displacement along them. As an important geological structure, fractures are well known as their geometry is critical for rock engineering design. Because joints have been formed by definite stress and regimes, they tend to crop up in sets with definite orientations (Sakran, 2016). As the Aheimer Formation is highly fractured, joint data have been collected using one-dimensional (1D) line sampling (scan-lines), following the Priest's method (Priest, 1993), where the sampling needs a well-exposed planar rock face. Each scan-line was marked by a measuring tape and ranged from 40-70 m long. Scan lines were set up perpendicular to fractures in order to diminish the directional sampling prejudice. In addition, the circle-inventory method (Titley, 1976; Davis, 1996) has been used in many stations where a circle with a diameter of 3 m is traced out on the bedrock surface of completely exposed fractured rock. Data sampled along each scan line and circle include orientation, spacing, persistence, length, roughness, aperture, and filling (Fig. 4). Trends of faults and fractures were graphically represented using Stereonet 9 (Allmendinger, 2012) in the form of rose diagrams (i.e. 2D form). In addition, fracture orientation data were graphically presented in 3D form using stereograms. Furthermore, major joint sets have been used for the kinematic analysis of slope instabilities by means of the stereographic projection technique (Hoek, 1981; Goodman, 1989; Wyllie & Mah, 2004). Wedge and toppling failure styles were kinematically studied. Wedge failure takes place where the intersection of the main joints is positioned in the area between the slope face and the great circles representing the angle of internal friction (Φ). Toppling failure is based on a two dimensional relationship ($90 - \delta + \Phi < \alpha$) where δ = dip of discontinuity, Φ = friction angle of the discontinuity and α = slope angle. Wyllie et al., 2004 concluded that it is possible to resolve the stability conditions of a slope on the same stereonet using a combined kinematic analysis (i.e., analyze daylight envelopes). In addition, the stability conditions are possibly determined according to the relationship between daylight envelopes and pole points (Gischig et al., 2011).

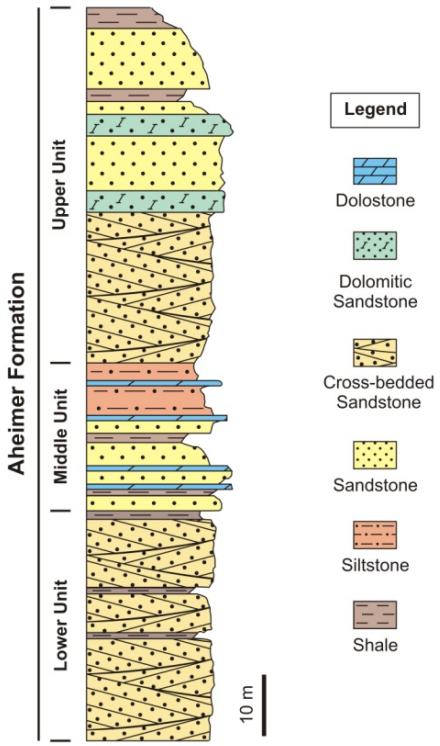

Fig. 5 Stratigraphic column showing the lithological composition of the Aheimer Formation.

Geotechnical data

The geotechnical properties were investigated for the exposed rock mass in the study site using both field observations/measurements and laboratory tests (Fig. 4). Detailed geotechnical studies were carried out to determine the engineering geological characteristics of the rock mass using the Rock Mass Rating (RMR). Twenty-five undisturbed samples were collected from the study site for laboratory testing. Firstly, a visual description of rocks was identified in the field classified according to ASTM D 2488, 2009. Secondly, the parameters of the discontinuities, spacing, roughness and aperture of discontinuities were determined in accordance with the ISRM methods (ISRM, 1981). Further, for the laboratory works, the engineering properties of the intact rock mass and rock mass were considered. Subsequently, the physical properties of the rocks, including density and water absorption were determined according to (ASTM D6683, 2014; ASTM D6473,

2015). To achieve the complete geotechnical qualification, the Rock Mass Rating (RMR) system (Bieniawski, 1989) was carried out, including the Rock Quality Designation (RQD). RQD was calculated according to (Palmstrom, 1982) by using data of major discontinuity sets in twelve stations was chosen according to the field observations in discontinuities sites.

$$RQD = 115-3.3\ (Jv) \quad (1)$$

Using data of major discontinuity sets in twelve stations. It can be measured from the joint set spacing with a volume of the rock mass as, Where, Jv is the sum of the number of joints per (m3). Also, intact rock material's compressive (crushing) strength was measured in dry conditions (ASTM C170M, 2017). Finally, the geotechnical results were analyzed in order to propose the geotechnical qualification and judgment of the geotechnical properties of rocks in the study site.

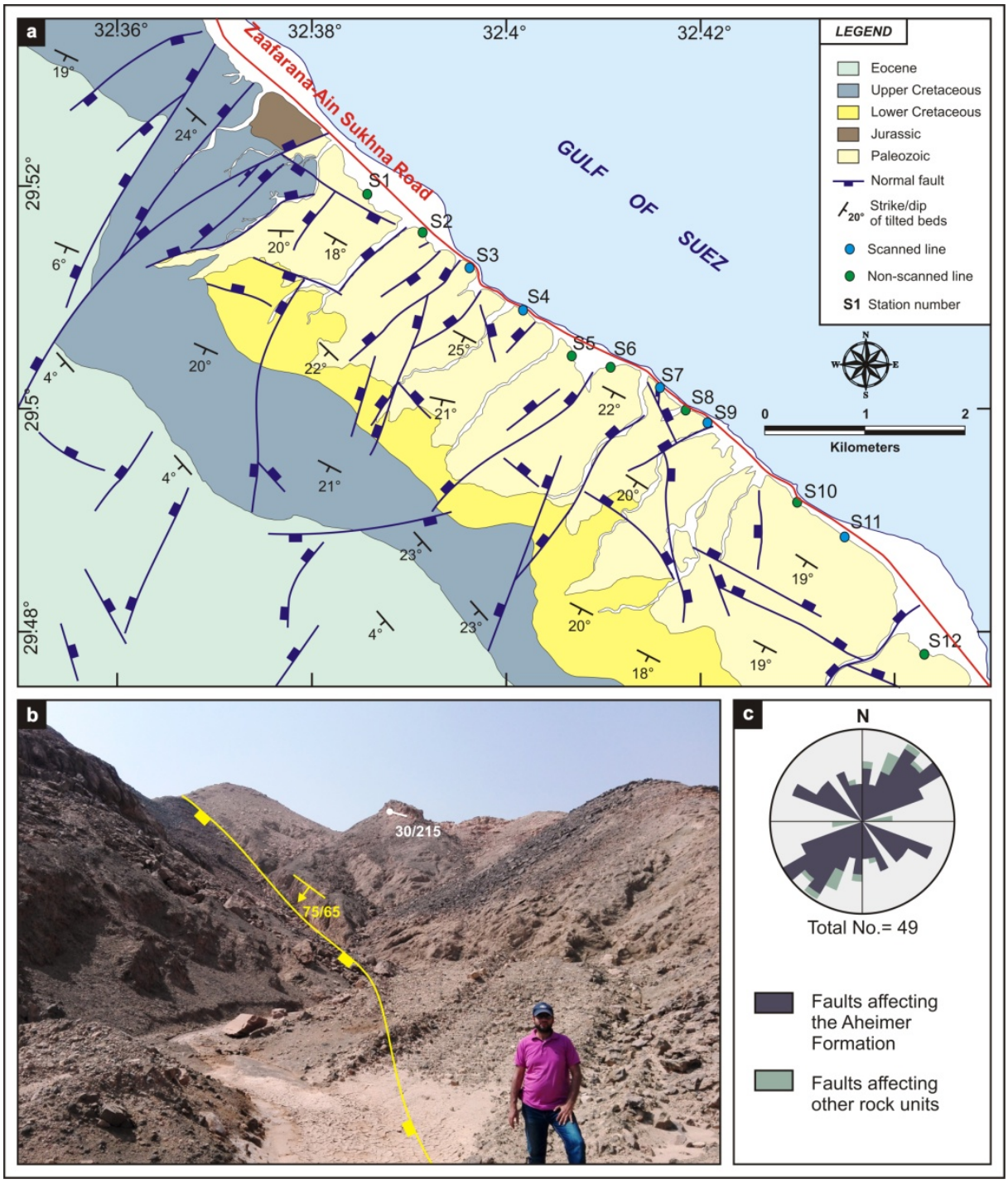

Fig. 6 (a) Geological map based on interpretation of satellite images and fieldwork of the study area showing the main lithological units and major faults in the study area. Blue and green circles represent locations of collected joint data. (b) Field photo for a striking normal fault that cut the Aheimer Formation, looking towards SSW. (c) Rose diagram of the mapped faults at the study area.

Results and discussion

Structural setting

In the study site, faults are clearly exposed throughout the whole area. Where found, fault surfaces are characterized by dip-slip kinematic indicators, which show normal displacement. The measured dip data from many fault surfaces indicated a moderate to steep angle, which usually ranges from 65 to 75º. A total of 49 faults were mapped in the study area, including 32 faults that dissect the foundation bedrock (Fig. 6). Faults are frequently surrounded by a narrow damage zone consisting of fractured sandstone. In addition, a small number of faults exhibit fault cores that enclose a zone of fine-grained cataclastic rocks, which are 1 m wide in some localities. The mapped faults belong to three prominent sets; NE-SW, NNE-SSW and WNW-ESE. In addition, three subordinate fault sets have infrequently represented by NNW-SSE, NW-SE and ENE-WSW directions (Fig. 6).

To inspect the geometrical parameters of fractures, twelve stations at various exposures of the sandstones of the foundation bedrock have been analyzed in detail. Quantitative descriptions and statistical distribution of fractures at the study site are given in Table 1. The collected data represent a total of 276 fractures. The measured orientations of the scanned fractures belong to five main discontinuity sets (Table 1) oriented in descending order of frequency; NW-SE (JS-1), NNW-SSE (JS-2), WNW-ESE (JS-3), ENE-WSW (JS-4) and NE-SW (JS-5), (Fig. 7a). The measured dip values of the investigated fractures show moderate to high dip values ranging from 50 to 90° for JS-1, while most of the other sets exceed 75° (Fig. 7b). Most of the studied fractures are perpendicular to sub-perpendicular to bedding planes and intersect each other. Conjugate fractures are very well represented by JS-1, JS-3 and JS-2 along the exposed studied rock unit (Fig. 7c), especially near-fault surfaces. On the other hand, vertical or sub-vertical, parallel fractures have been well observed in JS-1, JS-2 and JS-5 (Fig. 7d, e).

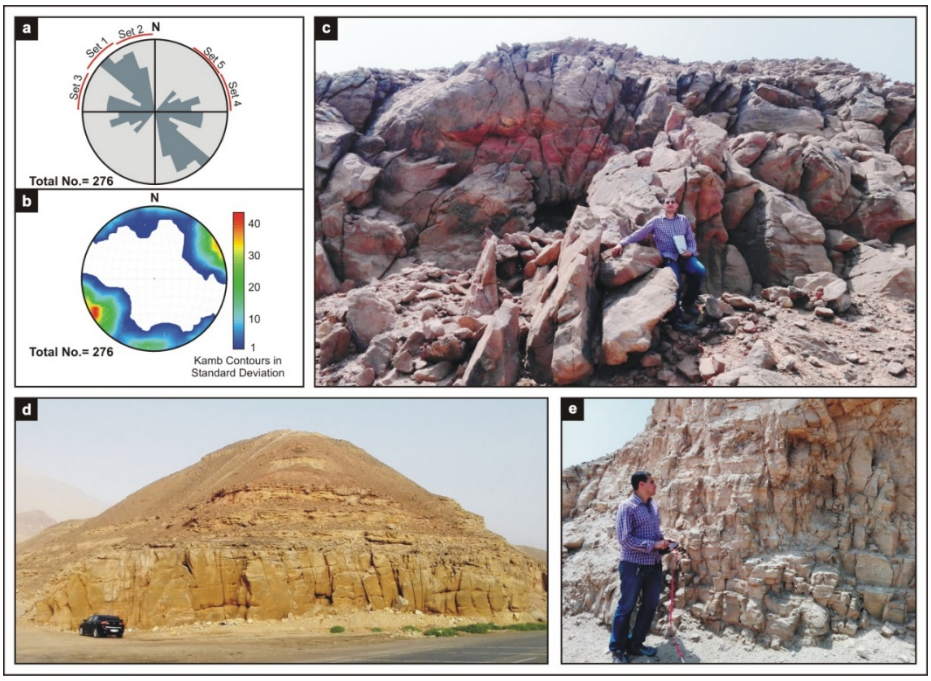

Fig. 7 (a) Rose diagram for strike orientations of the collected fracture data from the Aheimer Formation. (b) Stereoplots of poles to fractures that were measured in the field. (c) Field photo showing steeply-dipping conjugate fractures, looking towards SW. (d) Field photo of vertical fractures that reach 3 m length and measure 0.5-1 m spacing, looking towards WNW. € Field photo of closed-spaced, short joints wit a low degree of persistence, SW.

Generally, the mean spacing of the measured joints ranges from 0.42 to 0.89 m (Table 1). The maximum joint spacing can be observed in JS-3 as it attains 2.8 m, whereas JS-5 represents the minimum joint spacing as it does not exceed 1 m. Most of the studied joints have dry joint surfaces and are rarely damp. They exhibit a moderate persistence (12.98- 46.7 cm); however, persistence was found to exceed 150 cm in some stations, especially in JS-1, JS-2 and JS-3 (Table 1). Joints are generally filled with cohesive fine sediments or occasionally without filling (Table 1). Their width is 1.45 to 15.55 cm, but it was found to exceed 50 cm in some localities in JS-1 and JS-2. Fracture length ranges from 0.4 to 3.2 m (Fig. 7). The maximum joint lengths are very well represented by JS-1 and JS-2, while JS-5 represents the minimum joint lengths (Table 1). The

roughness of the examined discontinuities shows, in usual, smooth undulating, occasionally rough stepped joint surfaces.

Further, fractures associated with a selected fault zone have been investigated in order to assess rock quality in areas affected by fault zones (S7, Fig. 6). This was accomplished by a detailed joint survey along both the hanging wall and the footwall of the fault (Fig. 8). The width of the fault zone is around 1 m. The mean orientation, in descending order, for 56 measured fractures along the hanging wall is NW-SE and NNE-SSW (Fig. 8). Whereas the orientations are NNW-SSE and ENE-WSW for 43 fractures measured along the footwall (Fig. 8). In general, fractures are short in length and are closely spaced, especially near the fault zone, with very low persistence. In addition, shear fractures are common along the hanging wall. The dip angles of the measured fractures along both sides of the fault zone are steep and range from 75 to 90°.

Fracture Set	No.	(Strike/Dip)	Length (m)	Spacing (m) min-max/ average	Roughness	Aperture (cm) min-max/ average	Filling	Persistence (cm) min-max/ average	Water Condition	Weathering
JS-1	104	321/74	3.2	0.1-1.8/0.66	A	0-70/15.55	*	0-150/37.5	Dry joint surface	Slightly weathered
JS-2	66	340/83	2.86	0.2-1.3/0.72	B	0-50/9.5	**	0-200/46.7	Dry joint Surfaces, occasionally damp	Moderately Weathered
JS-3	50	282/84	0.92	0.2-2.8/0.89	C	0-20/8.25	***	0-150/64	Dry joint Surfaces, occasionally damp	Moderately Weathered
JS-4	44	079/80	1.1	0.15-1.4/0.65	D	0-8/2	****	0-60/13.10	Dry joint Surfaces, occasionally damp	Moderately Weathered
JS-5	12	050/90	0.4	0.5-0.97/0.42	D	0-5/1.45	****	1-70/12.98	Dry joint Surfaces, occasionally damp	Slightly weathered

Tab. 1. Quantitative descriptions and statistical distribution of fractures at the study site.

A	Generally smooth undulating, occasionally rough stepped	*	Generally thick filling (cohesive material and in some cases fine sediments), occasionally without filling
B	Generally rough stepped, occasionally smooth undulating	**	Generally without filling, occasionally thick filling (cohesive material) and fine sediments
C	Generally rough stepped	***	Generally fine sediments, occasionally thick filling (cohesive material and, in some cases, without filling
D	Generally smooth undulating	****	Generally without filling

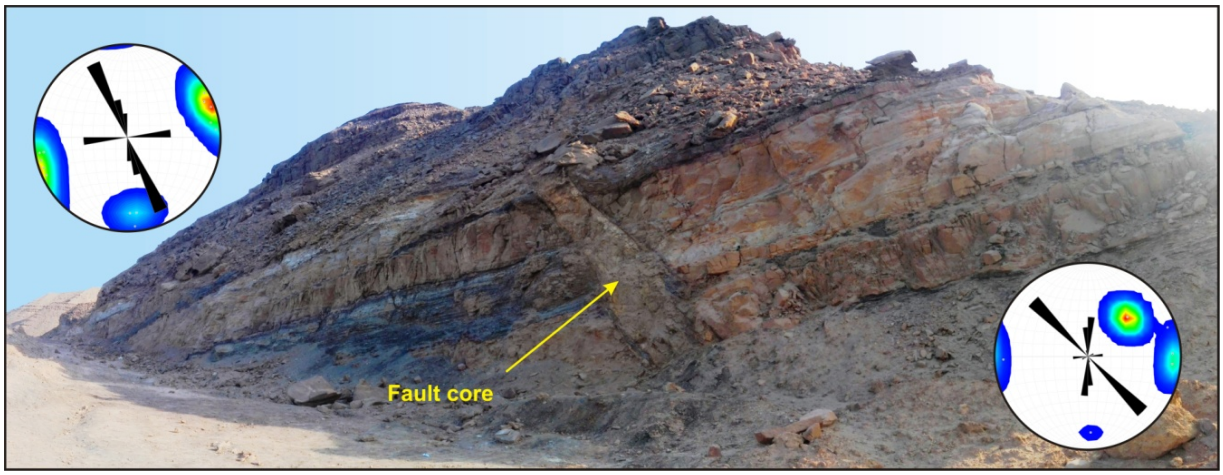

Fig. 8 The studied fault zone at station 7 (S7). Rose diagrams of the measured fracture orientations and stereo plots of poles to fractures are represented for the hanging wall (right) and footwall (left).

Kinematic analysis of fracture data

The properties of discontinuities such as orientation, roughness, filling and persistence represent a significant control on the quality of a rock mass and stability of rock slopes. In addition, the strength of the whole rock mass is mainly controlled by discontinuities and weathering. The study of geological and mechanical considerations in terms of rock mass classification systems is favorable to specifying the definite properties of

the rocks forming the slope and to provide a preliminary evaluation of the slope stability. Consequently, this, in turn, can be critical consideration in avoiding geo-engineering and geo-environmental troubles.

In the light of the abovementioned, kinematic analysis of rock slope is assessed to determine the influence of the discontinuities on stability and to identify possible modes of failure in the light of the relationship between the orientation of the resultant discontinuity sets and the face (Table 2).

Tab. 2. Geometr455arameter susedsed in the kinematic analysis.

Station No.	Joint sets	Joint set dip direction/ dip	Slope direction/ angle	Slope Height (m)
2	JS-2	70/85	70/85	18
	JS-4	354/73		
3	JS-1	52/73	70/85	26
	JS-4	354/73		
8	JS-1	52/73	30/85	35
	JS-2	70/85		
	JS-3	11/83		
9	JS-1	52/73	40/80	16
	JS-2	70/85		
	JS-3	11/83		

Herein, the predefined joint sets have been recalled for the kinematic analysis and geometrical characteristics of slope instabilities at the lower slope of the studied rock unit facing the Zaafarana-Ain Sukhna Road (Figs. 6 and 9). According to field observations and data measurements, only four stations at sandstone exposures of the foundation bedrock have local and limited slope failures. In the present study, slope faces and the main joint sets have been plotted as great circles for the four studied stations (i.e. S2, S3, S8 and S9) (Fig. 9). In addition, a combined kinematic analysis was performed to plot and analyze joint orientation data for each station. The dip and dip directions of each joint set, as well as slope angles and directions, were determined to portray the daylight envelopes (Table 2 and Fig. 10). The internal friction angles of the discontinuity planes range from 30° to 35°, which have been used in the analysis of the current slopes in dry conditions (Figs. 9 and 10).

The analysis of these four stations according to field measurements and stereographic projection of joint sets revealed the presence of wedge as well as toppling failures (Figs. 9 and 10). At S3, wedge failure resulted from the intersection of JS-1 and JS-4. Also, wedge failure at S8 is a result of the intersection of JS-1, JS-2 and JS-3. On the other hand, toppling failure was common at S2 and S9 due to JS-2 and JS-1, respectively (Table 2).

Physical rock properties

Twenty-five samples were collected from the intact rock and the rock mass for the laboratory tests. The unit weight and water absorption of the intact rock and rock masses were determined according to ASTM D6683, 2014, ASTM D6473, 2015. The results are presented in Table 3. The values of the unit weight range from 2.14 to 2.76 kN/m^{3,} and the mean value is 2.38 kN/m^3. Also, in the present study, 15 cube samples were soaked for 48 hours to determine the water absorption, which ranged from 2.95 to 5.56 % and with a mean value of 4.2 % (Table 3).

Tab. 3. Material properties of Paleozoic sandstone of bedrock and joints.

Properties.	Test No.	Mean	Max	Min
Compressive Strength, (Mpa)	20	12.00	16.00	8.00
Compressive Strength, (Mpa)	20	12.00	16.00	8.00
Unit Weight (γ , kN/m3)	25	2.38	2.76	2.14
Water absorption (%)	15	4.20	5.56	2.95
Rock Quality Designation (RQD)%	overall 80.58%, occasionally in fault zone 40.53%			
Joint set number	Five major joint sets			
Spacing of discontinuities (m)	__	0.64	1.8	0.02
Aperture of discontinuities (cm)	Generally 0–70, occasionally tight			
Roughness of discontinuities	Generally smooth undulating, occasionally rough stepped			
Infilling	Generally hard filling, occasionally without filling			
Weathering degree	Generally moderately weathered, occasionally slightly weathered			

Compressive (Crushing) Strength

The strength of intact rock material was measured according to ASTM C170M, 2017. In addition, the strength of the stone is tested to determine its resistance to crushing and bending. The compressive strength was

determined in the dry conditions and with the load parallel or perpendicular to the rift. (Fig. 11). The resultant compressive (crushing) strength of the sandstone samples ranges from 8 to 16 Mpa, with a mean value of 12 Mpa (Table 3).

Rock quality designation (RQD)

According to Palmstrom (1982), the RQD was calculated by using five major discontinuity sets of data in twelve stations representing all differentiation in the study site (Figs. 6 and 7). The RQD was estimated totally for the highly fractured rock masses using data corresponding to the quantitative descriptions (Table 3). The obtained RQD values show the degree of deformation in the Paleozoic bedrock. The average value of the calculated RQD at the whole studied rock unit is 80.58 %, revealing that the bedrock has moderate to high rock quality. The RQD value for the inspected fault zone (S7) is 40.53 %, revealing fair rock quality in accordance with measurements of five major sets of discontinuities.

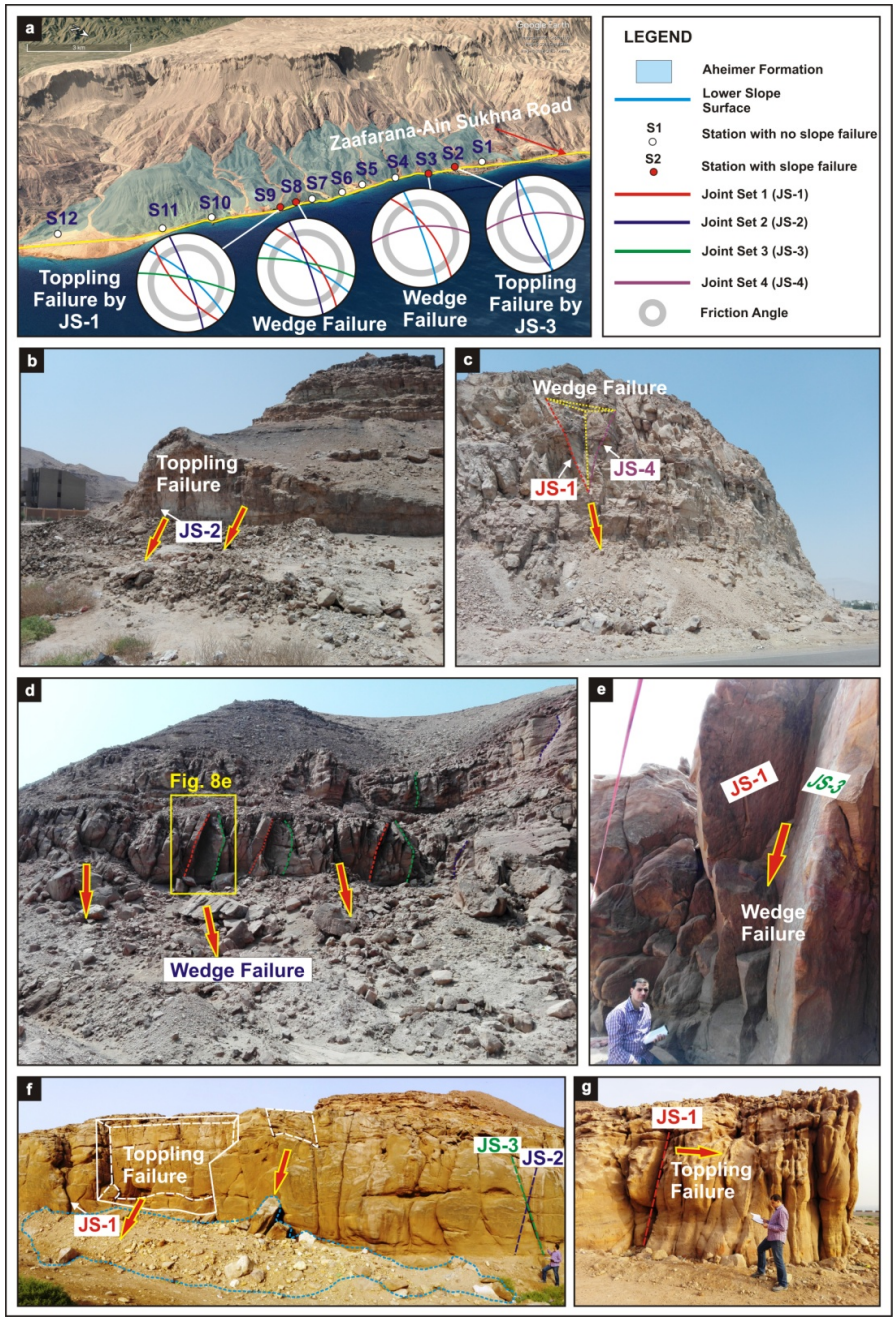

Fig. 9 (a) Kinematic analysis of joints and failure modes found in the studied rock unit. (b) Toppling failures at S2. (c) Wedge failure at S3. (d, e) Wedge failure at S8. (f, g) Toppling failure at S9.

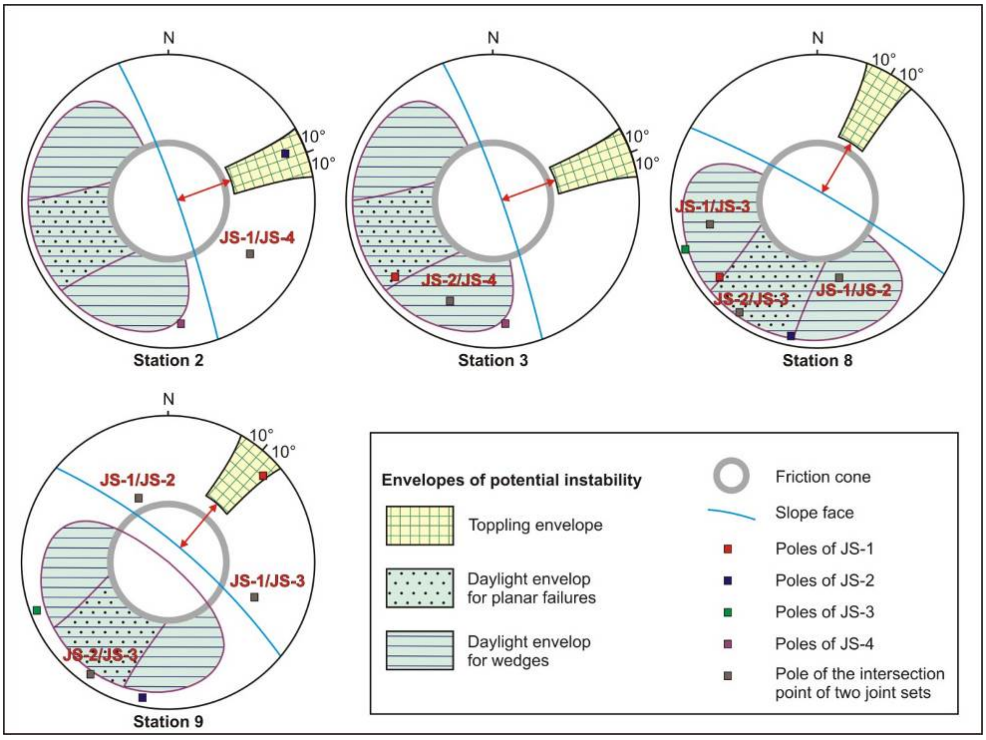

Fig. 10 The combined kinematic analyses for S2, S3, S8, and S9.

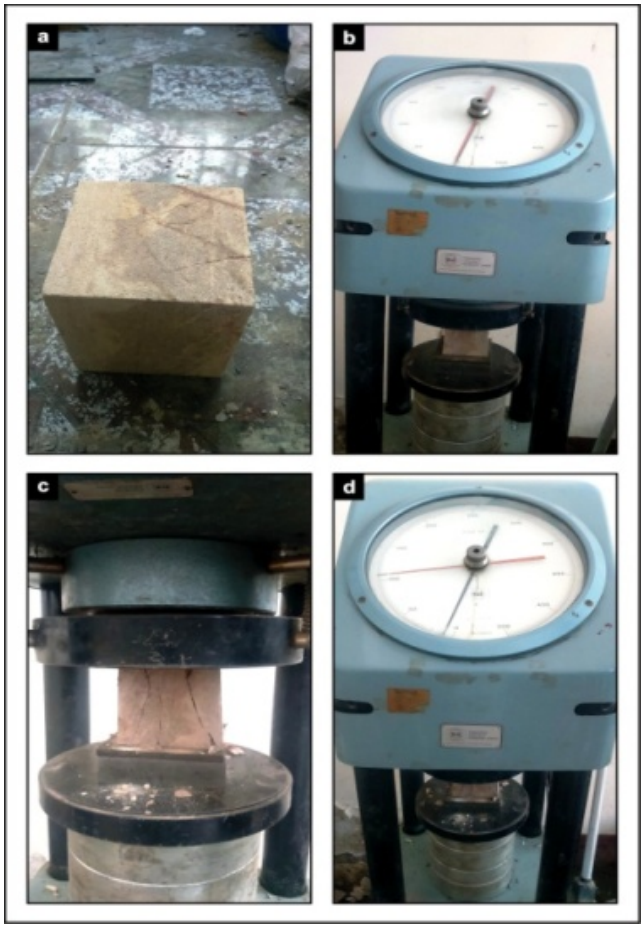

Fig. 11 Compressive (crushing) strength test (a&b before and c& d after test).

Tab. 3. Material properties of Paleozoic sandstone of bedrock and joints.

Properties.	Test No.	Mean	Max	Min
Compressive Strength, (Mpa)	20	12.00	16.00	8.00
Compressive Strength, (Mpa)	20	12.00	16.00	8.00
Unit Weight (γ , kN/m3)	25	2.38	2.76	2.14
Water absorption (%)	15	4.20	5.56	2.95
Rock Quality Designation (RQD)%	overall 80.58%, occasionally in fault zone 40.53%			
Joint set number	Five major joint sets			
Spacing of discontinuities (m)	__	0.64	1.8	0.02
Aperture of discontinuities (cm)	Generally 0–70, occasionally tight			
Roughness of discontinuities	Generally smooth undulating, occasionally rough stepped			
Infilling	Generally hard filling, occasionally without filling			
Weathering degree	Generally moderately weathered, occasionally slightly weathered			

Rock mass rating (RMR)

RMR system (Bieniawski, 1989) is used to evaluate the geotechnical condition of the whole bedrock. Also, RMR is used with a special focus on a selective fault zone in order to assess the effect of deformation on the bedrock. Table 4 gives the ratings for each of all the abovementioned parameters. The studied rock unit is characterized by compressive (crushing) strength that is ranged from 5-25 and a rating value of 2; the RQD ranges from 75- 90 %, where its rating value is 17. In addition, the spacing of discontinuities ranges from 200-600 mm with a rating value of 17. Subsequently, the guidelines for classification of discontinuity conditions using discontinuity length (persistence), separation (aperture), roughness, infilling (gouge) and weathering were carried out, and the sum rating values of these parameters are 20. Groundwater has also been assessed, where the studied rock unit is in completely dry conditions, with a rating of 15. The effect of discontinuity orientation is classed as favorable for tunneling, foundations and slopes where the rating value is -2. Hence, The RMR is classed from the total rating for the studied rock unit, where the value of RMR is 71. For the fault zone (S7), RMR has also been estimated, which is presented in Table 4. The selected fault zone is characterized by compressive (crushing) strength that ranges from 5-25 with a rating value of 2 with an RQD value that ranges between 25-50 %, where its rating value is 8. In addition, the spacing of discontinuities ranges from 60-200 mm with a rating value of 8. Subsequently, the guidelines for classification of discontinuity conditions using discontinuity length (persistence), separation (aperture), roughness, infilling (gouge) and weathering were carried out, and the sum ratings of these parameters is 18. According to groundwater assessment, the studied rock unit is in completely dry conditions with a rating value of 15. The effect of discontinuity strike and dip orientation was classed as favourable for tunnelling, foundations and slopes, where the rating value is -2. Hence, the RMR is classified from the total rating for the studied rock unit, where the value of RMR is 51. The abovementioned findings suggest that the Paleozoic sandstones of foundation bedrock are classified as good rock II category, with cohesion ranging from 300- 400 Kpa and has high friction angle ranging from 35-45°. Also, the RMR for the fault zone is 51, which is classified as fair rock III category, with lower friction angle ranges from 25-35° and cohesion from 200-300 Kpa, according to Bieniawski, 1989.

Tab. 4. The Rock Mass Rating (RMR) system (Bieniawski, 1989), for Paleozoic sandstone

Item	Value	Rating	Fault zone
Compressive test	12	2	2
RQD	75 - 90 %, 25-50 %	17	8
Spacing of discontinuities	0.64 cm	15	10
Condition of discontinuities	____	24	18
Groundwater	Completely dry	15	15
Adjustment for joint orientation	Drive with dip-Dip 20-45º (favorable)	-2	-2
	Total	71	51

It is clear that the resultant discontinuity analysis agrees with the RMR result that shows the suitability of the bedrock for construction. However, the kinematic analysis shows the presence of some failure modes at a few stations at the lower slope of the rock. Thus, these results reveal that the deformation in the form of discontinuities and the dip directions could not lead to instability problems and less probability of various

problematic conditions during and after construction processes. However, attention must be paid during the expansion and extension of roads near fault zones as well as slope failures.

Consequently, the results urge that the initial design and construction stage is favourable to utilize the support suggested for fair rock. Moreover, it is possible to gradually reduce the support requirements if the construction is progressing well with no stability problems.

Conclusions

The present work concerned the assessment of structural and geo-engineering characteristics of Paleozoic sandstones, which are exposed at the eastern scarp of the Northern Galala Plateau, facing the Zaafarana- Ain Sukhna Road. Since faults and fractures are the predominant structures in the studied area, structural elements and geotechnical properties of the rock mass exposed in the study site were investigated using both field observations/measurements and laboratory tests. The analysis of 12 stations from different exposures at the Aheimer Formation showed that only four stations registered wedge and/or toppling failures. Geotechnically, the RQD results revealed that most of the studied rock unit is characterized by moderate to high rock quality. Contrarily, the RQD results at the studied fault zone revealed fair rock quality in accordance with measurements of five major sets of discontinuities. Accordingly, RMR values suggest that the majority of the investigated locations of the foundation bedrock are classified as the good rock II category, whereas RMR for the fault zone is classified as the fair rock III category. Finally, it is meaningful to declare that the resultant kinematic discontinuity analysis and the Rock Mass Rating system revealed the suitability for most of the constructions at the bedrock. However, precautions should be considered specifically near fault zones as well as slope failures. Therefore, the present study opens the way for more in-situ geo-engineering and seismicity investigations for fault risk assessment during various construction operations and development processes.

References

Abdallah, A.; Adindani, A. Stratigraphy of Upper Paleozoic rocks, western side of the Gulf of Suez. Egyptian Geological Survey, Egypt, 1963, 25, pp. 18.

Abd-Elaty, I.; Pugliese, L.; Zeleňáková, M.; Mésároš, P.; Shinawi, A.E. Simulation-based solutions reducing soil and groundwater contamination from fertilizers in arid and semi-arid regions: Case study the eastern nile delta, Egypt. International Journal of Environmental Research and Public Health 2020, 17(24), pp. 1–18.

Abd-Elshafy, E.; Abd-El-Azeam, S. Paleogeographic relation of the Egyptian Northern Galala with the Tethysduring the Cretaceous Period. Cretac Res 2014, 31, pp. 291-303.

AbouElenean, K.M.; Mohamed, A.M.E.; Hussein, H.M. Source parameters and ground motion of the Suez-Cairo shear zone earthquakes, Eastern Desert, Egypt. Nat Hazards 2010, 52, pp. 431-451.

Al Far, D.M. Geology and coal deposits of Gebel Maghara, north Sinai, Egypt. Egyptian Geological Survey, Egypt, 1966, 37, pp. 59.

Alfvén, L. Structural and Engineering Geological Investigation of Fracture Zones and Their Effect on Tunnel Construction. Published at Department of Earth Sciences, Uppsala University (www.geo.uu.se), Uppsala, 2015; pp. 78.

Allmendinger, R.W.; Cardozo, N.C.; Fisher, D. Structural Geology Algorithms: Vectors & Tensors: Cambridge, England, Cambridge University Press, 2012, pp. 302.

ASTM C170/C170M-17. Standard Test Method for Compressive Strength of Dimension Stone, ASTM International, West Conshohocken, PA, 2017. Available online: www.astm.org.

ASTM D 2488-09a. Standard practice for description and identification of soils (visual-manual procedure). ASTM International, West Conshohocken, PA, 2009. Available online: www.astm.org.doi:10.1520/D2488-09A

ASTM D6473-15. Standard Test Method for Specific Gravity and Absorption of Rock for Erosion Control, ASTM International, West Conshohocken, PA, 2015. Available online: www.astm.org.

ASTM D6683-11. Standard test methods for measuring density. ASTM International, West Conshohocken, PA, 2014. Available online: www.ASTM.org.doi:10.1520/D6683-11.

Attwa M.; Henaish, A. Regional structural mapping using a combined geological and geophysical approach - A preliminary study at Cairo-Suez district, Egypt. J Afr Earth Sci 2018, 144, pp. 104-121. Available online: https://doi.org/10.1016/j.jafrearsci.2018.04.010

Attwa, M.; Shinawi, A. E. Geoelectrical and geotechnical investigations at tenth of Ramadan city, Egypt - A structure- Based (SB) model application. Near Surface Geoscience 2014- 20th European Meeting of Environmental and Engineering Geophysics, 2014.

Attwa, M; Henaish, A. Zamzam, S. Hydrogeologic characterization of a fault-related dome Using outcrop, borehole and electrical resistivity data. Natural Resources Research 2020, 29(2), pp. 1143-1161. Available online: https://doi.org/10.1007/s11053-019-09504-6

Bieniawski, Z.T. Engineering Rock Mass Classification. Wiley, Chichester, 1989, pp. 251.

Boukhary, M.; Kenawy, A.; Basta, R. Early Eocene Nummulitids from Gebel Umm Russeies, El Galala El Bahariya, Eastern Desert, Egypt. Geologia Croatica 2019, 62/1, pp. 1-18.

Davis, G.H.; Reynolds, S.J. Structural Geology of Rocks and Regions. Wiley, New York, 1996.

Diet Maio, R.; Paola, C.; Forte, G.; Urciuoli, G. An integrated geological, geotechnical and geophysical approach to identify predisposing factors for flowslide occurrence. Engineering Geology 2020, 267, 105473. Available online: https://doi.org/10.1016/j.enggeo.2019.105473

Du, J.; Yin, K.; Glade, T.; Woldai, T.; Chai, B.; Xiao, L.; Wang, Y. Probabilistic hazard analysis of impulse waves generated by multiple subaerial landslides and its application to Wu Gorge in Three Gorges Reservoir, China. Engineering Geology 2020, 276, 105773. Available online: https://doi.org/10.1016/j.enggeo.2020.105773

Duffy, B.; Campbell, J.; Finnemore, M.; Gomez, C. Defining fault avoidance zones and associated geotechnical properties using MASW: a case study on the Springfield Fault, New Zealand. EngGeol 2014, 183, pp. 216-229. Available online: http://dx.doi.org/10.1016/j.enggeo.2014.10.017.

El Shinavi, A.; Naymushina, O. S. Geotechnical aspects of flood plain deposits in south east Aswan City, Egypt. ARPN J Eng. Appl. Sci. 2015, 10 (8), 3490-3497.

El Shinawi, A, Ramadan, F and Zelenakova, M (2021). Appraisal for the environment, weathering and provenance of Upper Cretaceous-Lower Tertiary shales, Western Desert, Egypt. Acta Montanistica Slovaca, 171-184, doi.org/10.46544/AMS.v26i1.15

El Shinawi, A. Instability improvement of the subgrade soils by lime addition at Borg El-Arab, Alexandria, Egypt. J. Afr. Earth Sci 2017, 130, pp.195-201.

El Shinawi, A.; Mésároš, P.; Zeleňáková, M. The Implication of Petrographic Characteristics on the Mechanical Behavior of Middle Eocene Limestone, 15th May City, Egypt. Sustainability 2020, 12 (22), 9710.

Farouk, S. Upper Cretaceous sequence stratigraphy of the Galala Plateaux, western side of the Gulf of Suez, Egypt. Mar Pet Geol 2015, 60, pp. 136-158. Available online: https://doi.org/10.1016/j.marpetgeo.2014.11.005

Ghorab, M.A. Abnormal stratigraphic feature in RasGharib oil field. 3rd Arab Petrol Congr, Alexandria, 1961, pp. 10.

Gischig, V.; Amann. F.; Moore, J.R., Loew, S.; Eisenbeiss, H.; Stempfhuber, W. Composite rock slope kinematics at the current Randa instability, Switzerland, based on remote sensing and numerical modeling. Eng Geol 2011, 118, pp. 37-53.

Goodman, R.E. Introduction to rock mechanics, 2nd ed., Willey, New York, 1989, pp. 576.

Hack, H.R.K.; Price, D.G. Determination of discontinuity friction by rock mass classification. Proc 8th Int. Sco. Roc. Mech. (ISRM) Congress, Tokyo, Japan, 1995, pp. 23-27.

Henaish, A. Fault-related domes: Insights from sedimentary outcrops at the northern tip of the Gulf of Suez rift, Egypt. Mar Pet Geol 2018, 91, pp. 202-210. Available online: https://doi.org/10.1016/j.marpetgeo.2018.01.009

Henaish, A.; Attwa, M. Internal structural architecture of a soft-linkage transfer zone using outcrop and DC resistivity data: Implications for preliminary engineering assessment. EngGeol 2018, 244, pp.1-13. Available online: https://doi.org/10.1016/j.enggeo.2018.07.018.

Henaish, A.; Kharbish, S. Linkage style of rift-associated fault arrays: insights from central Cairo-Suez district, Egypt. Carpathian Journal of Earth and Environmental Sciences, 2020, 15(1), pp. 189 - 196. Available online: DOI:10.26471/cjees/2020/015/121

Hoek, E.; Bray, J.M. Rock slope engineering. Institute of Mining and Metallurgy, London, 1981.

Hussein, I.M.; Abd-Allah, A.M.A. Tectonic evolution of the northeastern part of the African continental margin, Egypt. J Afr Earth Sci 2001, 33, pp. 49-68.

International Society for Rock Mechanics ISRM. Point load test, suggested method for determining point load strength. Int J Rock Mech Min SciGeomechAbstr 1985, 22, pp. 55-60.

International Society for Rock Mechanics ISRM. Rock characteri¬zation, testing and monitoring. In: Brown ET (Ed), ISRM Suggested Methods, Pergamon Press, Oxford, 1981, pp. 211.

Ishii, E. Preliminary assessment of the highest potential transmissivity of fractures in fault zones by core logging. Eng. Geol. 2017, 221, pp. 124-132. Available online: http://dx.doi.org/10.1016/j.enggeo.2017.02.026.

Kang, Y.; Liu, Q.; Xi, H., Gong, G. Improved compound support system for coal mine tunnels in densely faulted zones: A case study of China's Huainan coal field. Eng. Geol. 2018, 240, pp. 10-20. Available online: https://doi.org/10.1016/j.enggeo.2018.04.006.

Koleini, M.; Van Rooy, J.L. Falling rock hazard index: a case study from the Marum Dam and power plant, south-western Iran. Bull Eng. Geol. Environ 2010, 66, pp 483-492.

Kramarenko, V.V.; El Shinawi, A.; Matveenko, I.A.; Shramok, A.A. Clay swelling of Quaternary and Paleogene deposits in the south-eastern flanks of West Siberian iron ore basin. IOP Conference Series: Earth and Environmental Science, 2016, 33(1), 012041.

Krenkel, E. Geologie Afrikas. Bornträger, Berlin, 1925, pp. 461.

Leia, Q.; Lathama, J.P.; Xianga, J.; Tsangb. C.F. Role of natural fractures in damage evolution around tunnel excavation in fractured rocks. Eng. Geol. 2017, 231, pp. 100-113. Available online: http://dx.doi.org/10.1016/j.enggeo.2017.10.013.

Moustafa, A.R.; Khalil, M.H. superimposed deformation in the northern Suez Rift, Egypt: relevance to hydrocarbons exploration. J Petroleum Geol 1995, 18, pp. 245-266.

Naymushina, O.S.; Shvartsev, S.L.; Zdvizhkov, M.A.; El-Shinawi, A. Chemical characteristics of swamp waters: A case study in the Tom River basin, Russia. Water-Rock Interaction - Proceedings of the 13th International Conference on Water-Rock Interaction, 2010, WRI-13, 955–958

Özsan, A.; Öcal, A.; Akin, M.; Başarır, H. Engineering geological appraisal of the Sulakyurt dam site, Turkey, Bull Eng. Geol. Environ 2007, 66, pp. 483-492.

Palmstrom, A. The volumetric joint count - A useful and simple measure of the degree of rock mass jointing. IAEG Congress, New Delhi, 1982, pp. 221-228.

Peng, F.L.; Qiao Y.K.; Sabri, S. A collaborative approach for urban underground space development toward sustainable development goals: Critical dimensions and future directions. Front. Struct. Civ. Eng. 2021, 15, 20-45. Available online: https://doi.org/10.1007/s11709-021-

Priest, S.D. Discontinuity Analysis for Rock Engineering. Chapman & Hall, London, 1993, pp. 473.

Said, R. Planktonic Foraminifera from Thebes Formation, Luxor, Egypt. Micropaleont 1960, 6, pp. 277-286.

Said, R. The Geology of Egypt. Balkema, Rotterdam, 1990, pp. 734.

Sakran, S.; Nabih. M.; Henaish. A.; Ziko, A. Fracture reopening by micro-earthquakes, a mechanism for oil seepage in mildly active rifts: a case study from Gemsa oilfield, the southern Gulf of Suez rift, Egypt. Arab J Geosci 2016, 9, pp. 404.

Sari, M. Incorporation of uncertainty in estimating the rock mass uniaxial strength using a fuzzy inference system. Arab J Geosci 2019, 12, pp. 18. Available online: https://doi.org/10.1007/s12517-018-4169-z

Sawires, R.; Peláez, J.A.; Ibrahim, H.A.; Helbary, R.; Henares, J.; Hamdache, M. Delineation and characterization of a new seismic source model for seismic hazard studies in Egypt. Nat Hazards 2016, 80, pp. 1823-1864.

Schütz, K.I. Structure and stratigraphy of the Gulf of Suez, Egypt. In: Landon SM (Ed) Interior rift basins, AAPG Memoir 1994, 59, pp. 57-96.

Shahar, J. The Syrian arc system: an overview. Palaeogeogr., Palaeoclimatol., Palaeoecol. 1994, 112, pp. 125–142, 5 figs., Amsterdam.

Shang, J.; Hencher, S.R.; West, L.J. Tensile Strength of Geological Discontinuities Including Incipient Bedding, Rock Joints and Mineral Veins. Rock Mech Rock Eng 2016, 49, pp. 4213–4225. Available online: https://doi.org/10.1007/s00603-016-1041-x

Titley, S.R. Evidence for a Mesozoic linear tectonic pattern in southeastern Arizona. Arizona Geological Society Digest 1976, 10, pp. 71-101.

Toké, N.A.; Boone, C.G.; Arrowsmith, J.R. Fault zone regulation, seismic hazard, and social vulnerability in Los Angeles, California: Hazard or urban amenity. Earth's Future 2014, 2, pp. 440-457.

Wyllie, D.C.; Mah, C.W. Rock slope engineering: civil and mining, 4th ed., Spon Press, Taylor and Francis Group, London, 2004, pp. 431.